Upper Limits on the Presence of Ring Systems Around Long-Period *Kepler* Giant Planet Candidate KOI-422

Presented in Partial Fulfillment of
the Requirements for the Degree of

Master of Science

with a Major in

Physics

in the

College of Graduate Studies

University of Idaho

by

William Timothy Hatchett IV

april 2015

Major Professor
Jason W. Barnes, Ph.D

Committee
Matthew Hedman, Ph.D
Christine Berven, Ph.D
Department Chair
Jo Ellen Force, Ph.D

Authorization to Submit Thesis

This thesis of William Timothy Hatchett, submitted for the degree of Master of Science with a Major in Physics and titled "Upper Limits On the Presence of Ring Systems Around Long-Period *Kepler* Giant Planet Candidate KOI-422," has been reviewed in final form. Permission, as indicated by the signatures and dates below, is now granted to submit final copies to the College of Graduate Studies for approval.

Major Professor:	Jason W. Barnes, Ph.D	Date
Committee Members:	Christine Berven, Ph.D	Date
	Matthew Hedman, Ph.D	Date
Department Chair:	Jo Ellen Force, Ph.D	Date

Abstract

Is Saturn alone in the universe or are there other planets out there with stunning ring systems like Saturn's? To discover that Saturn is not alone would help us to learn more about the formation and evolution of Saturn's ring system, and about ring systems as a whole as well. We show a process to determine which star-planet pairs might be easiest to search for the presence of rings. We then look for exorings around transiting exoplanet candidate KOI-422.01 by examining the residual of a best fit line assuming that no ring system exists. After the residual was examined, we re-fit KOI-422.01 to determine if a spherical fit exhibits a better fit than a ringed model various ring size and orientation. It was determined that a spherical fit matched the light curve of KOI-422.01 better than a light curve with obliquity angles 90°, 60°, 45°, or 20°. We find no evidence for rings around KOI-422.01, but the methods that we have developed can be used for more comprehensive ring searches in the future.

Acknowledgements

We thank Dr. Matt Hedman for answering any questions regarding Saturn's rings. Also I'd like to thank Dr. Christine Berven for being on my comitte. Also a big thanks to Shannon MacKenzie and Johnathon Ahlers for their useful comments.

Dedication

To my Mother and beautiful Wife who have been there for me since I started school. To my Father who has also been through the turmoils of graduate school. Also thanks to my family and step father for the encouragement they gave me to finish my degree.

Table of Contents

List of Tables

List of Figures

CHAPTER 1

Introduction

Rings and disks play an important role at many scales of the universe: from galactic planes to protoplanetary disks to rings around planets. Within our own solar system, rings appear to be a common phenomenon, but different rings have very different characteristics. Jupiters rings, for example, were first seen from a backlit image by Voyager 1 (Owen *et al.*, 1979). Neptune's rings were first detected using stellar occultation, but because they do not have a consistent density around Neptune it was unclear if that planet really had rings until they were imaged by Voyager 2 (Cruikshank and Matthews, 1995). Neptune's rings are difficult to see because they are very dark (Cuzzi, 1985). Uranus has more dense rings than both Jupiter and Neptune but they are also dark and difficult to see, so they were first detected using an occultation (Elliot *et al.*, 1977), then later viewed in 1986 by Voyager 2 (Smith *et al.*, 1989). Saturn, of course has the most extensive ring system, which has been studied by observers since before 1655 and first viewed in 1610 by Galileo Galilei (Galilei, 1989). Maxwell (1856) first showed that these rings were composed of particles rather than a solid disk.

Not only do all the giant planets in our solar system have rings, but we are finding that smaller bodies in the solar system can have rings as well. Recently rings were discovered around Centaur 10199 Chariklo (Braga-Ribas *et al.*, 2014) and, Chiron (Ortiz *et al.*, 2015; Ruprecht *et al.*, 2015; Thiessenhusen *et al.*, 2002), which confirms that solid bodies can also have ring systems. These discoveries suggest that rings may be more common than previously recognized.

Outside of our solar system, a 'ring' type system was found around stellar companion J1407b, as reported by Mamajek *et al.* (2012). This ring system was found to have a radius on the order of 0.6 AU (Kenworthy and Mamajek, 2015). Because of the size of the J1407b disk system, it is more likely to represent a protosatellite disk than it is to be an exoring system, because the radius of this disk is larger than the Roche limit of a planet. In that case, the particles associated to J1407b disk would inevitably

coalesce into moons. However this discovery reinforces the idea that disk systems are common in the universe and that we can detect them with current instruments.

Ultimately, it is still unclear how rings form around planets, how long they remain stable, or how they dissipate. There are several hypotheses that have been proposed to explain the formation of rings. Some possible mechanisms for the formation of Saturn's rings are that they are remnants from the formation of the solar system, that they are formed from comets being ripped apart by tidal forces, or tidal disruption of satellite formation in the early solar system (Pollack *et al*., 1976; Harris, 1984; Canup, 2010; Dougherty and Esposito, 2009). Some rings are formed by impact or volcanic processes ejecting particles off of moons into orbit around the planet (Tiscareno, 2013), such as, Saturn's E ring (Spahn *et al*., 2006).

Saturn's main rings are much more complex than any other in our solar system, and they appear to be composed of mostly water-ice (Pilcher *et al*., 1970). This composition gives them their high albedo. Saturn's rings also have an unknown age (Cuzzi *et al*., 2010). Saturn's rings could be as old as the solar system, but this idea must than somehow explain the purity of the water-ice in the rings (Cuzzi and Estrada, 1998). Alternatively they could be as young as, or younger, than 4.4 million years old (Northrop and Connerney, 1987). Even after 400 years of research, how Saturn's rings formed and evolve remains poorly understood.

With the onset of exoplanet discoveries exoplanet ring searches became a logical next step. Barnes and Fortney (2004) showed that it is possible to detect Saturn-like rings using *Kepler* transits. Arnold (2005) showed how light curves are affected by artificial objects occulting the Sun. Ohta *et al*. (2009) demonstrated how to detect rings using light curves or radial velocity methods.

This work constrains the likelihood of observing large Saturn-type ringed planets via *Kepler* transit light curve detection. Section 2 explains our process for choosing the planetary candidates most likely to have rings. A description of how these stellar systems are modeled and analyzed to determine the presence of rings is explained in section 3. In section 4, we show how our model simulates the planet-ring transits. Section 5 summarizes our results. Finally, Section 6 discusses some conclusions and possible implications about finding exoplanetary ring systems.

CHAPTER 2

Candidate Selection

In this initial attempt to constrain the presence of rings around exoplanets, we focus on the best candidates. To that end, we select for *Kepler* Objects of Interests (KOI) (1) that we think have the highest probability to possess a rings system and (2) that have the highest quality *Kepler* photometry so that we can place a meaningful constraints on the exoplanet. To find ringed exoplanet candidates, we search in the Mikulski Archive for Space Telescopes (MAST) database for certain criteria for each KOI. These criteria are: long orbital periods, a high signal-to-noise ratios (SNR), large radii, and large ice Roche limits.

Long period orbits are prefered because we want candidates that reside beyond the ice line where water-ice can form. As shown in Hedman (2015) it may be that large Saturn-type rings require a composition of primarily ice. Unfortunately, *Kepler* was unable to discover any candidates that have a periods $\gtrsim 4.4 yrs$, which is the distance of the ice line for Sol (Hayashi, 1981). However, rings could potentially be composed of rock and reside inside the ice line (Schlichting and Chang, 2011). We can not be sure that a ring system made of rock will be large enough, due to a Roche Limit smaller than ice. It then seems reasonable to assume that rings not made primarily of water-ice might be difficult to detect (Arnold and Schneider, 2004). In the presence of this restriction, we choose KOI's with orbital periods ≥ 100 days, with the longest periods preferred.

We required a SNR $\gtrsim 100$. Thus, we can detect ring anomalies in the residual from ring occultation. As we will discuss in section 3, the presence of rings is predominantly detectable in photometry during ingress and egress of the planet-ring system.

A good candidate will have a large inferred radius. Zuluaga *et al*. (2015) showed that a ringed planet will appear larger than it should due to the presence of rings. Thus abnormally large initial-guess planet radii can also be an indication of rings. An example of this is imagine if an observer viewed Saturn from another star system. The

KOI	289.02	422.01	1353.01	3541.01
$R_p\,(R_{Jup})$	0.63	1.3	1.0	1.1
$M_p\,(M_{Jup})$	0.5	0.8	1	1
Period (days)	296.653	809.014	125.865	421.428
$\mathcal{R}_{ice}\,(R_{Jup})$	2.73	2.45	2.64	2.64
$\mathcal{R}_{rock}\,(R_{Jup})$	1.89	1.70	1.83	1.83
$\frac{\mathcal{R}_{ice}}{R_p}$	4.64	1.82	2.66	1.84
$\frac{\mathcal{R}_{rock}}{R_p}$	3.21	1.26	1.84	1.83

TABLE 2.1: Roche Limits for planetary candidates KOI-289.02, KOI-422.01, KOI-1353.01, and KOI-3541.01 with ice or rock particles. Periods are in days, planet radii, and Roche values are in Jupiter radii. The planet radius and mass are established from Fortney *et al*. (2007). Errors associated with the period are $< \pm 0.001$. Errors associated with Roche limits are $\pm$ 0.1 which is attributed primarily to the mass estimate as other errors are negligible in comparison.

observer would initially deduce the radius of Saturn to be twice as large as the true radius due to the rings (Tusnski and Valio, 2011). This scenario is expected to happen with us as the interstellar observer. Therefore, we eliminate all candidate with radii less than 0.5 R_{Jup}.

If a planet candidate has a small Roche limit then, the rings orbiting that planet would be too small to detect. We assume that any ring system will lie inside its planets Roche limit. Therefore, we calculate the Roche limit of the remaining candidates using the equation

$$\mathcal{R} \approx 2.45 R_p (\frac{\rho_p}{\rho})^{\frac{1}{3}} \tag{2.1}$$

where R_p is planet radius, ρ_p is the planets density, and ρ is the particle density (Carroll and Ostlie, 1996). Figure 7 of Fortney *et al*. (2007) was used to assign a mass, based on a probable radius, to each planet candidate. The Roche limit was than calculated using $\rho = 1 g/cm^3$ (ice), and $\rho = 3 g/cm^3$ (rock).

These criteria allowed us to select four of the KOIs on which to focus: KOI-289.02, KOI-422.01, KOI-1353.01, and KOI-3541.01.

I

CHAPTER 3

Data

We obtained *Kepler* photometry from the publicly available MAST database. We processed the data before evaluating it for the absence or presence of exorings. After cleaning the data we fit each planet candidate as a spherical body to determine if there is probable cause to search for exorings.

3.1 DATA REDUCTION

Our planetary reduction methods were kept to a minimum to ensure that we did not introduce any artifacts. First we filtered the data with a median box filter. The filter box is $\gtrsim 3$ times the length of the transit duration to keep the transits unaffected.

As the ingress and egress of the light curve are imperative to the detection of rings we determine the orbital period manually. The orbital period was determined by folding the data, using the period provided by NASA Exoplanet Archive, then adjusting the orbital period as needed to obtain an accurate value for the period. An appropriate fold will align the midpoint of one transit with the midpoint of all other transits. We did not bin the long-cadence data to ensure we did not smear the critical ingress and egress data.

3.2 SPHERICAL FITS

To model our ringed planets we initially evaluate them as spherical planets using `transitfitter` (Barnes and Fortney, 2004). The spherical fit will determine the planet and star radius, impact parameter (b), and eccentricity (ϵ), but the fit will determine an improper planet radius if there really are rings. These fits will be used to search for residual anomalies, like those predicted by Barnes and Fortney (2004). We also use these values as initial guesses for ringed models in section 4.

Upon fitting each planet candidate, we examine the residuals to determine if anomalies are present. The characteristics that we are looking for in the residual

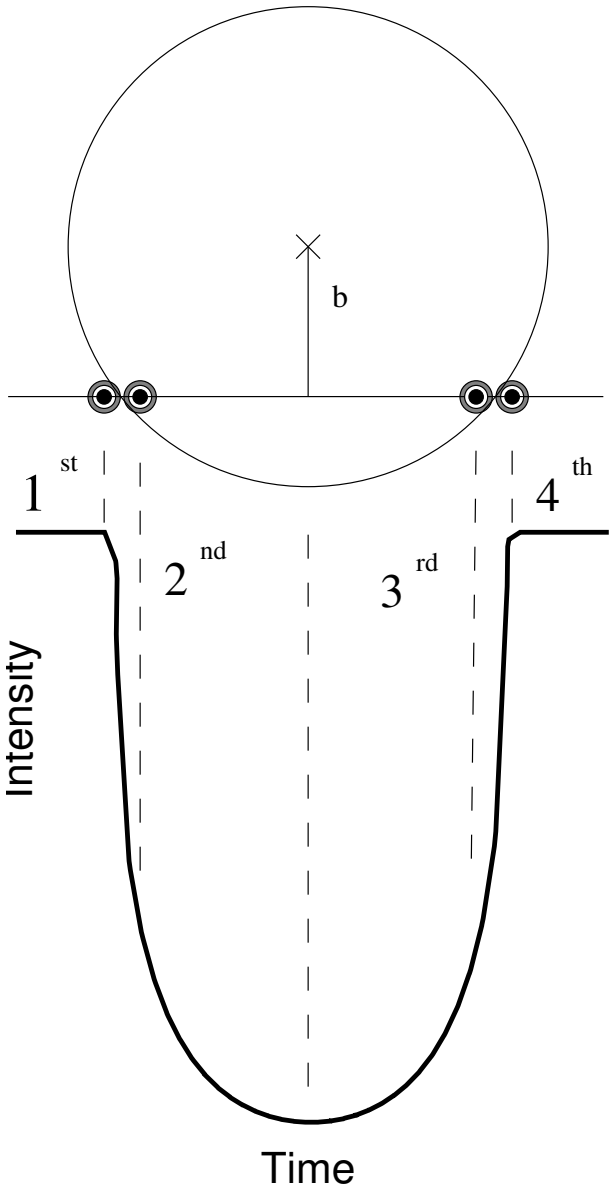

FIGURE 3.1: Illustration of 1st - 4th contact points on light curve and transiting bodies. 1st contact is the point at which the planet/ring first touches the star, causing the initial decline in luminosity. 2nd contact is once the trailing end of the planet crosses the stellar limb. This causes a change in inflection of the light curve. 3rd and 4th contact are 2nd and 1st contact in reverse respectively.

are best seen between 1^{st} and 2^{nd} contact (ingress), then again between 3^{rd} and 4^{th} contact (egress). These contact points are illustrated in Figure 1. We can see the expected anomalies, indicating rings, in Figure 6 for various angles. As seen for an obliquity (open) angle of 45° the residual will initially be higher than expected. Then near the midpoint of the ingress the residual becomes negative and eventually returns to an expected value. After the midpoint, the residual will slightly drop negative then become a positive residual to a negative residual returning to zero as the planet passes the last contact point.

The results from fitting these candidates as a spherical model are shown in Table 2 with our best fit lines and their residuals being displayed in Figures 2 through 5. Table 2 displays the star temperature of each of these candidates, from these temperature we are able to roughly estimate the value of the stellar mass. KOI-289, KOI-422, and KOI-1353 were set to have a mass of 1.1 $M_{\odot}$ and KOI-3541 was set to a mass of 1.2 $M_{\odot}$. The limb darkening coefficients for each KOI was defined by Sing (2010). All other values on Table 2 are fit for.

As seen in Table 2 both KOI-289.02 and KOI-1353.01 have radii smaller than Jupiter. These radii do not rule out rings around them, but do make them less desirable as fitting candidates. KOI-422.01 and KOI-3541.01, on the other hand, have a larger planet radius than would be expected for cold giants ($R_p \lesssim 1.1$).

Upon exploring the residuals of the four candidates we discover that all candidates have a flat residuals. The flat residual makes it probable that these candidates either have no rings or undetectable rings. Either because there are no rings, their rings are too small, or obliquity angle is too low, we were not able to detect rings with this method.

The radii of KOI-422.01 and KOI-3541.01 make them the best candidates to test for Saturn-type rings. The purpose of this paper is to uncover the feasibility of detecting Saturn-type rings around exoplanets, therefore only one of these two candidates will be evaluated. KOI-422.01 is being used because it has a longer orbital period and because it is less likely to be a brown dwarf or companion star due to KOI-3541.01 exceptionally large initial guess radius.

KOI	289.02	422.01	1353.01	3541.01
Temp. (K)	5951 ±180	6242 ±165	6279 ±171	6235 ±189
$R_s\,(R_\odot)$	1.34 ±0.08	1.34 ±0.04	1.00 ±0.02	0.99 ±0.08
$R_p\,(R_{Jup})$	0.634 ±0.04	1.72 ±0.06	1.02 ±0.03	2.85 ±0.24
b	0.21 ±0.087	1.95 ±0.04	0.41 ±0.027	0.76 ±0.10
ϵ	0	0.69 ±0.01	0	0.55 ±0.06
c_1	0.64	0.6221	0.6221	0.6221
c_2	0	0.0175	0.0175	0.0175
χ^2	1.98	1.19	1.45	7.64

TABLE 3.1: Paramaters of spherical model fit. Star mass are 1.1 $M_\odot$ for KOI-289, KOI-422, and KOI-1353 and 1.2 $M_\odot$ for KOI-3541. Temperatures are in Kelvin, R_s are in solar radii, R_p are in Jupiter radii, b is the impact parameter, ϵ is eccentricity, c_1 and c_2 are the first two limb darkening coefficients, and χ^2 is the statistical distribution test. Coefficients for stars limb darkening are obtained from Sing (2010) Table 2, and Stellar temperatures are obtained from CFOP (Community Follow-up Observing Program). Planetary systems with $\epsilon = 0$ were not fit for eccentricity because a circular orbit fit well.

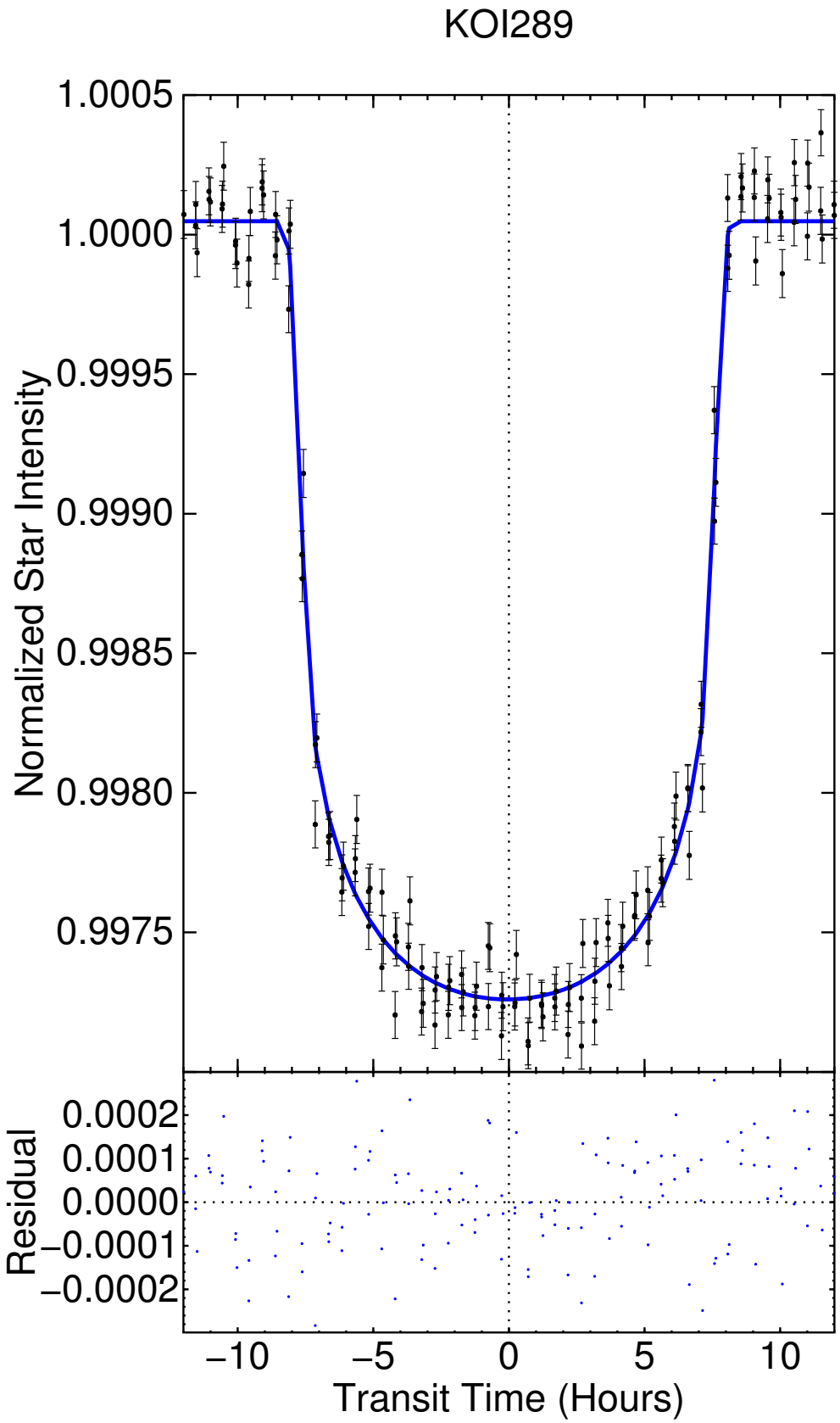

FIGURE 3.2: KOI-289 spherical fit (top) and residual (bottom).

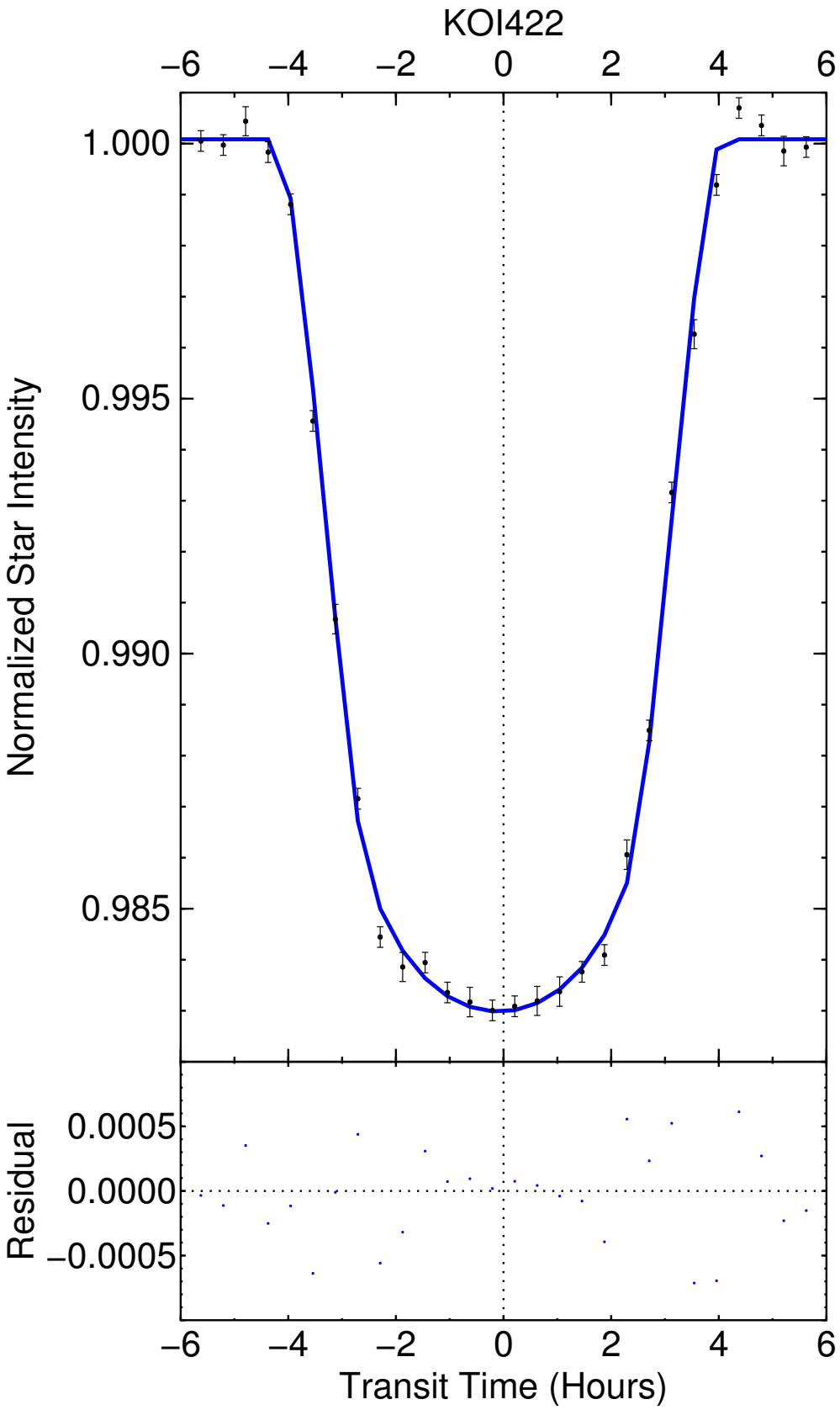

FIGURE 3.3: KOI-422 spherical fit (top) and residual (bottom).

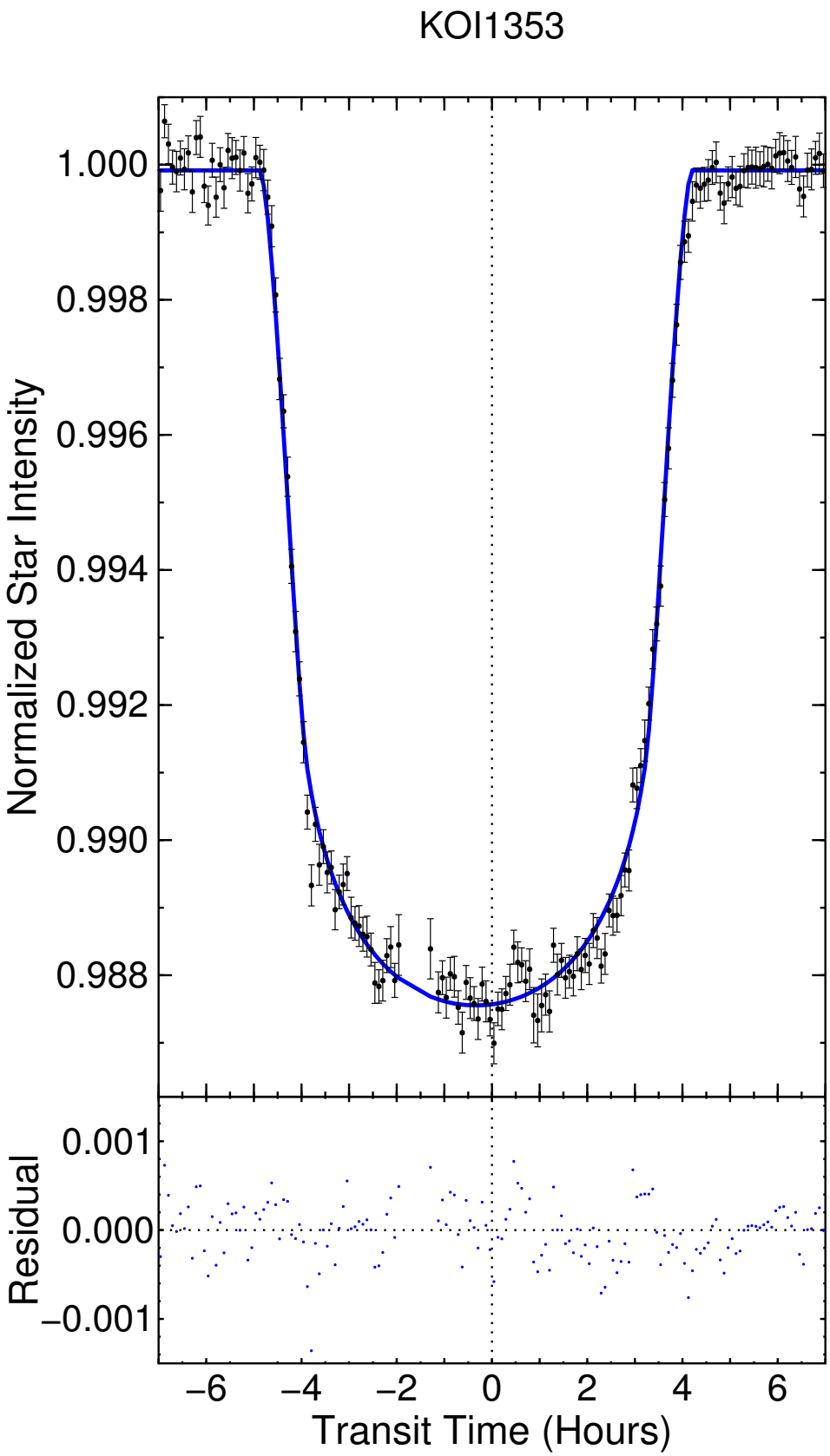

FIGURE 3.4: KOI-1353 spherical fit (top) and residual (bottom).

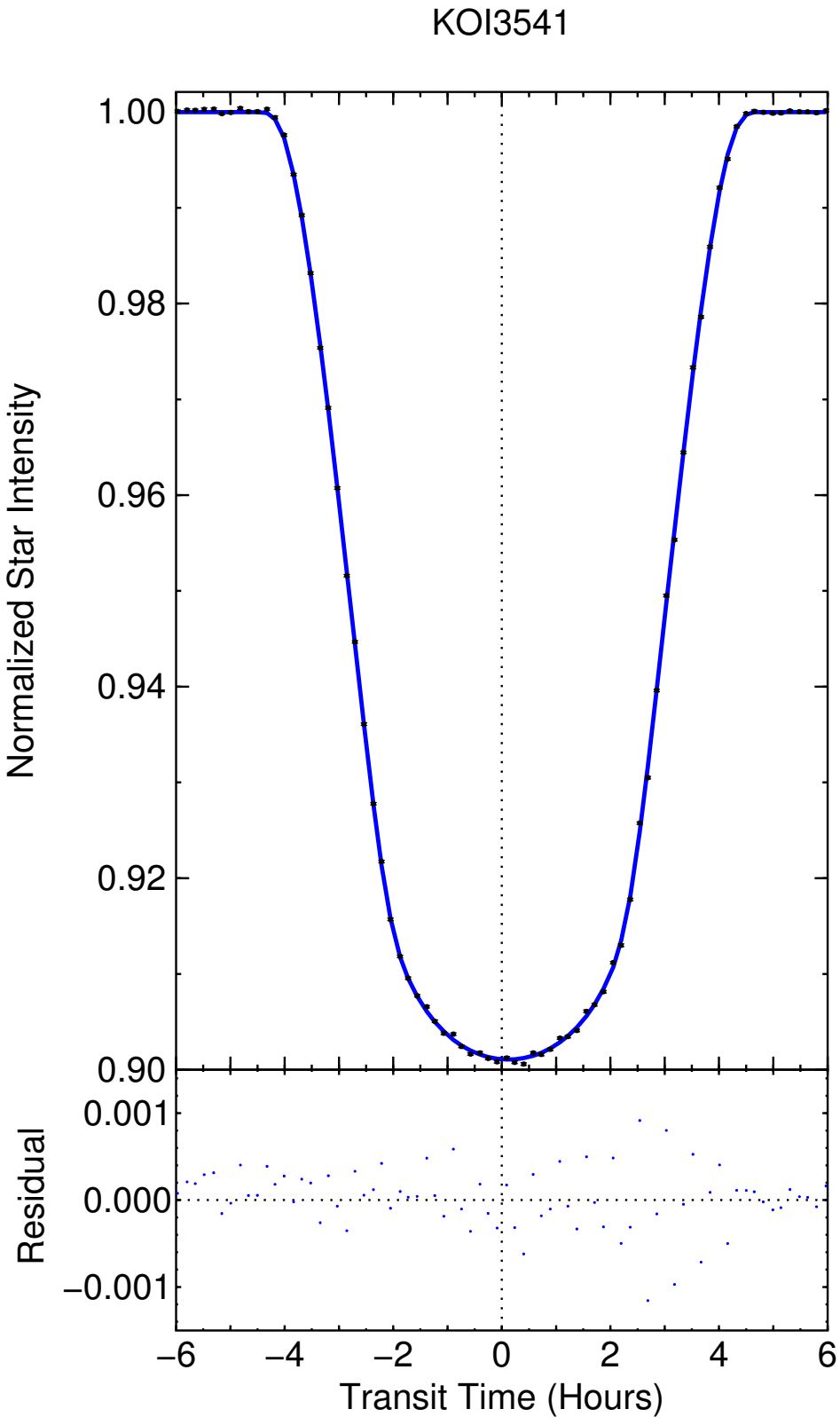

FIGURE 3.5: KOI-3541 spherical fit (top) and residual (bottom).

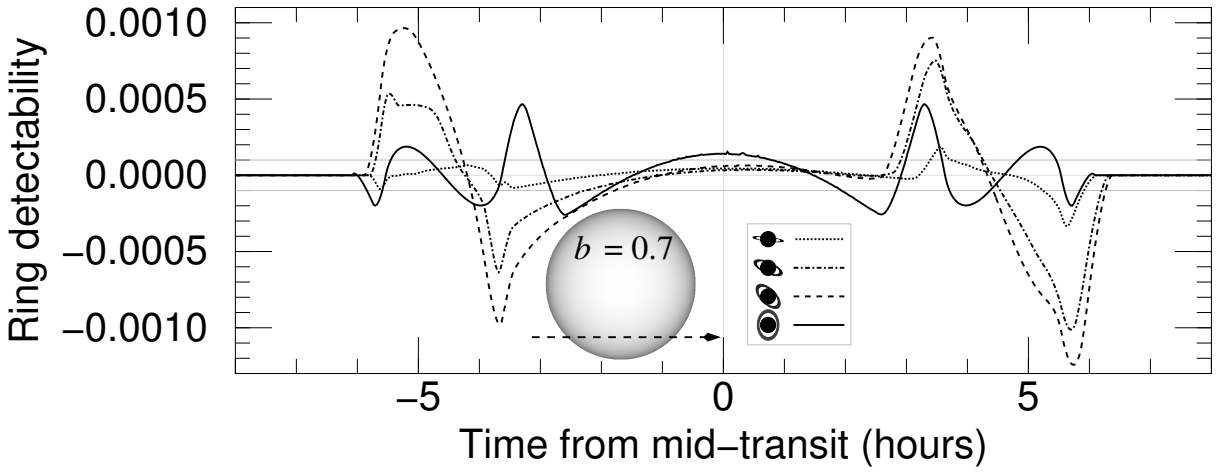

FIGURE 3.6: Theoretical ring detectability of a spherical body by residual; from Barnes and Fortney (2004). With azimuth angle and impact parameter set to $\pi/4$ and 0.7 respectively. Opening ring angles of 10° (dotted line), 30° (dashed-dotted line), 45° (dashed line), and 90° (solid line; face-on).

CHAPTER 4

Model

We use `transitfitter` (Barnes and Fortney, 2004) to produce synthetic light curves by simulating a spherical planet occulting a spherical star. The light curve is generated by taking a moment in time and integrating the total stellar flux blocked by the planet. It then repeats this for every instant in the planet's orbit.

When `transitfitter` is applied to a ring system, the rings is placed in the Laplace plane. As shown in Burns *et al*. (1979), the Laplace plane close to a planet is very near the equatorial plane, thus the model places the ring around the equator of the exoplanet.

4.1 Model parameters

Generalized orientations of rings requires the model to compensate for the different effects of each geometry on light curves. Our model allows the adjustment of five ring parameters listed below and shown in Figure 7.

1. Inner ring radius (R_i)
2. Outer ring radius (R_o)
3. Normal optical depth (τ)
4. Obliquity (ϕ)
5. Azimuth angle (ψ)

The inner radius is the distance from the center of the planet to the inner edge of the ring. The outer radius, likewise, is the distance from the center of the planet to the outer edge of the ring. The difference between these is the size of the rings as determined by the fit.

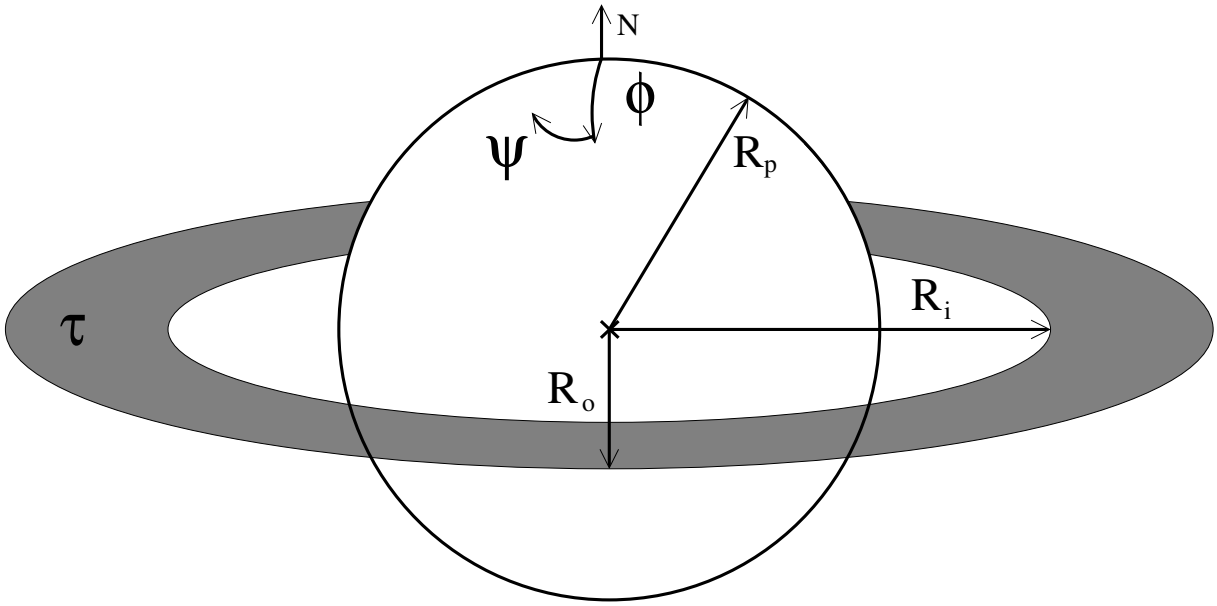

FIGURE 4.1: Angles definitions obliquity (ϕ), azimuth (ψ), R_o is outer radius of rings R_i is inner radius of rings R_p is radius of the planet.

There is a broad range of normal optical depth τ from the known ring systems in our solar system. Because τ is not the same for Jupiter as it is for Saturn, it becomes necessary to also allow for variety in our exoplanet candidates.

The obliquity, ϕ, is 90° when the north pole is pointed towards Earth. When $\phi = 90°$, the light curve will be symmetric about the mid-transit point, as shown in Figure 6. The azimuth angle, ψ, is the angle describing how far clockwise or counterclockwise the north pole is from the celestial plane. A rotation in ψ will have no effect on the light curve if $\phi = 0°$ or 90° because the position of the north pole is unaffected; however, the equatorial angle will change the ingress and egress of the light curve at any other value of ϕ.

4.2 RING MODEL EVALUATION

In this work we only consider whether a planet has large Saturn-type rings. Our model cannot detect the presence of small or diffuse rings; large, opaque rings are necessary to differentiate a ring system from a spherical body. Because of this limitation, we only constrain the largest a ring system can be to explain a light curve.

When fitting a ring system we hold τ, ψ, ϕ, R_p, and R_i constant. We hold τ constant because for any given ring system's light curve, as the same fit can typically be explained with a higher τ and lower ring radius or a lower τ and higher ring radius. For our initial guess we have defined $\tau = 1$; later iterations adjust τ to determine probable normal optical depth. Saturn's A and B rings have an average opacity of ≈ 2.5 (Nicholson, 2000), therefore, our search for exorings varies τ from 0.2 to 5. To determine the most likely orientation of the rings we fixed azimuth, ψ, to 90° and adjusted obliquity, ϕ, on various fits. The obliquity angles are set to 90°, 60°, 45°, and 20° for subsequent fits. These angles will determine the probable position for the rings.

In Fortney *et al*. (2007) it was demonstrated that the radius of a planet is related to the mass and distance from the star, we note from their work that all planet radii are $\lesssim 1.3\ R_{Jup}$, but cold as giants to be $\lesssim 1.0\ R_{Jup}$. Allowing us to hold $R_p = 1$ when the spherical model indicates a radius larger than $\sim 1\ R_{Jup}$. Although, the planet radius could be less than 1, of course ,we choose this value because it is an easy number and any other radius chosen would also be a valid guess. To maintain realistic results, we include a gap between R_i and R_p, fixing the inner radius of the ring to be $1.1\ R_{Jup}$ (Estrada *et al*., 2015).

With τ, ψ, ϕ, R_p, and R_i held constant, the ring model is fit for outer ring radius, star radius, eccentricity, and impact parameter. The spherical model values are used for initial guess in the ring model.

The ring size and orientation will be determined by plotting reduced χ^2 vs. τ graph for the various ring angles and normal optic depth. Probable ring orientation and ring size is determined by lowest χ^2 value method.

CHAPTER 5

Results

Our results from the spherical model for all candidates show no significant residuals that might indicate the presence of a ring system. Therefore, we attempt to establish upper limits on rings surrounding one of our four candidates. We chose KOI-422.01 for the detailed calculations of upper limit. KOI-422.01 has a large initial guess planet radius determined by `transitfitter`, and it also has the longest orbital period of the four candidates. Because cold gas giants with radius larger than $\sim 1.0\ R_{Jup}$ (Fortney *et al.*, 2007; Seager *et al.*, 2007) cannot exist, we deduce that if KOI-422.01 is a planet, then it probably has rings. Also, with an orbital period of $\sim$ 809 days, it is less likely that the host star's gravity and radiance would adversely influence the planet's rings.

To first examine the possibility of an asymmetric transit, we check the fit for ring orientation having an obliquity $\phi = 45^\circ$ and azimuthal angle $\psi = 45^\circ$. The best-fit result using a spherical-planet model has $R_s = 1.1 \pm 0.03$, $R_o = 2.0 \pm 0.08$, $R_{ring} = 0.9\ R_{Jup}$, and $\chi^2_r = 4.99$. Such a high value of χ^2_r in relation to χ^2_{spher} indicates that any potential rings cannot deviate far from an azimuthal angle with the north pole pointing towards or away from us.

Because the most easily measured aspects of light curves are primarily a function of the total cross-sectional area of the transiting body, some light curves can be explained by multiple possible scenarios. For instance, if a ring system has an azimuthal or obliquity angle of 45° it would be indistinguishable from an angle of 135° or any iteration of 90°. To prevent degeneracy in fitting on a single light curve, we hold R_p, ψ, ϕ, R_i, and τ constant. We hold R_p constant at 1 R_{Jup} for KOI-422.01, assuming the highest possible planet radius as if this object were a ringed planet. Azimuth angle ψ is held constant because there is no evidence in the residual that suggest an asymmetry, therefore we hold ψ at 90° as this is the only angle that will result in a symmetric light curve. The obliquity angle ϕ is held constant on each fit, but we run separate fits with $\phi = 90^\circ$, 60°, 45°, and 20° to explore parameter space. We keep the inner radius of the ring constant to 1.1 R_{Jup} to retain a gap between the ring and

KOI-422.01				
Angle	90°	60°	45°	20°
$R_s\,(R_\odot)$	1.16 ±0.08	1.18 ±0.04	1.17 ±0.04	1.12 ±0.04
τ	1.	2.	5.	2
$R_o\,(R_{Jup})$	1.68 ±0.13	1.66 ±0.07.	1.77 ±0.07	2.30 ±0.12
b	1.82 ±0.09	01.87 ±0.04	1.86 ±0.05	1.78 ±0.05
ϵ	0.62 ±0.04	0.63 ±0.02	0.62 ±0.02	0.65 ±0.03
χ^2	1.38	1.31	1.30	1.26

TABLE 5.1: Ring Fit Parameters. Ring Fit Parameters for lowest χ^2 vs τ values. R_s in Solar radii and R_o in Jupiter radii.

planet as would result from atmospheric drag. The normal optical depth τ is held constant because a light curve with a larger ring system and lower optical depth will give the same results as a smaller ring system and higher optical depth, but we again assign varying values of τ on successive fits to explore its effects.

Given the constraint values above, we now fit for outer ring radius (R_o), star radius (R_s), eccentricity (ϵ), and impact parameter b. We fit to determine the most plausible orientation and size of a hypothetical rings surrounding KOI-422.01 using `transitfitter` fitting for R_s, ϵ, R_o and, b then adjust τ on subsequent fits. We then plot the resulting χ^2_r vs. τ as shown in Figure 8. We will then change obliquity ϕ, keeping azimuthal ψ constant, to ascertain a preferable orientation of the ring system.

Examining Figure 8, we can see that the a spherical model is favorable to any ring system around KOI-422.01. Therefore we interpret that if KOI-422.01 has rings, then they are undetectable using our method. Possible reasons that we might miss a ring could be that the gap between the simulated ring and planet was too large, which would increase the χ^2_r value. Or the rings might have a lower obliquity angle than was tested in this paper (i.e $\phi < 20°$), or the rings could be smaller in radial extent than we are able to detect with this method.

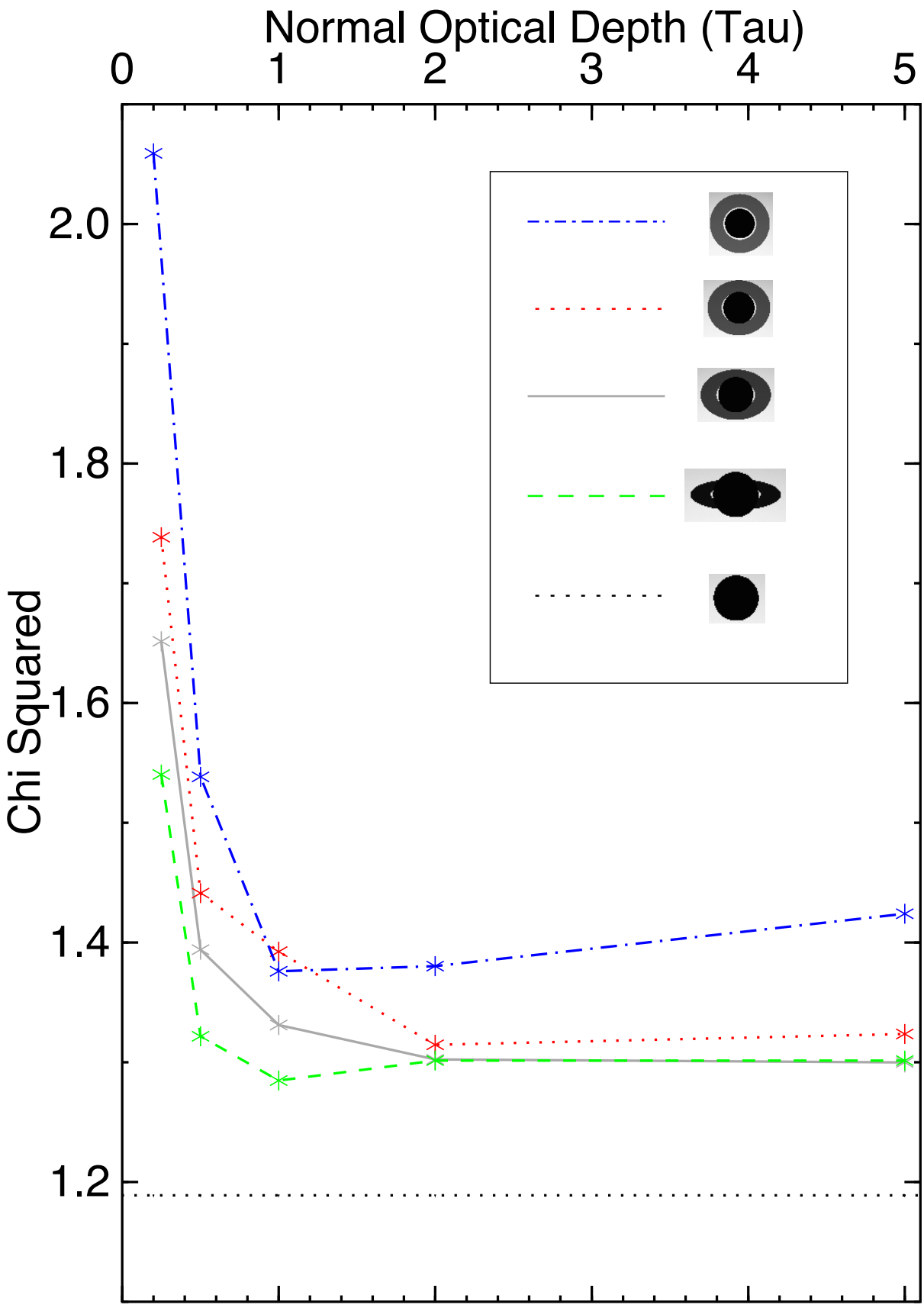

FIGURE 5.1: χ^2 as a function of τ. The resulting χ^2 for each obliquity angle ϕ as τ is adjusted. The blue dot-dashed line is $\phi = 90°$, red dotted line is $\phi = 60°$, grey solid line is $\phi = 45°$, green dashed line $\phi = 20°$, and black dotted line is a spherical fit for KOI-422.01.

chapter 6

Conclusion

In this initial pilot investigation to search for rings around exoplanets we have shown that KOI-422.01 is likely absent of large Saturn-type rings, by using a lowest χ^2 and residual methods. It is always possible however, that any of our four candidates possess a ring system that we cannot detect because the rings are too small, too transparent, or have a low obliquity angle (i.e., they are nearly edge on). It is also possible that none of these planets have rings. It is, perhaps, no surprise that KOI-422.01 does not have a detectible ring system given that it does not reside beyond the ice line of its host star. The implications of then planet's semi-major axis is that any rings around KOI-422.01 could not be made of ice.

To be able to answer fundamental questions of rings' origins and longevity, this pilot program would need to be expanded to search more for transiting planets ring candidates. Many questions can be answered once we find more potential exorings candidates, such as how long rings remain intact, and we can also get a better understanding of both the formation of rings and the formation of stellar systems (Barnes and Fortney, 2004). It seems reasonable to start a search for more exorings in the *Kepler* catalog. Once a large number of potential candidates have been found then perhaps some of these questions can be better understood.

Bibliography

Arnold L. and Schneider J. 2004. The detectability of extrasolar planet surroundings. I. Reflected-light photometry of unresolved rings. A&A420:1153–1162.

Arnold L.F.A. 2005. Transit Light-Curve Signatures of Artificial Objects. APJ627:534–539.

Barnes J.W. and Fortney J.J. 2004. Transit Detectability of Ring Systems around Extrasolar Giant Planets. APJ616:1193–1203.

Braga-Ribas F., Sicardy B., Ortiz J., Snodgrass C., Roques F., Vieira-Martins R., Camargo J., Assafin M., Duffard R., Jehin E., *et al*. 2014. A ring system detected around the centaur (10199) chariklo. Nature .

Burns J.A., Cuzzi J.N., Durisen R.H., and Hamill P. 1979. On the 'thickness' of Saturn's rings caused by satellite and solar perturbations and by planetary precession. AJ84:1783–1801.

Canup R.M. 2010. Origin of Saturn's rings and inner moons by mass removal from a lost Titan-sized satellite. Nature468:943–926.

Carroll B.W. and Ostlie D.A. 1996. An Introduction to Modern Astrophysics.

Cruikshank D.P. and Matthews M.S. 1995. Neptune and Triton. University of Arizona Press.

Cuzzi J.N. 1985. Rings of Uranus - Not so thick, not so black. Icarus63:312–316.

Cuzzi J.N., Burns J.A., Charnoz S., Clark R.N., Colwell J.E., Dones L., Esposito L.W., Filacchione G., French R.G., Hedman M.M., Kempf S., Marouf E.A., Murray C.D., Nicholson P.D., Porco C.C., Schmidt J., Showalter M.R., Spilker L.J., Spitale J.N., Srama R., Sremčević M., Tiscareno M.S., and Weiss J. 2010. An Evolving View of Saturn's Dynamic Rings. Science 327:1470–.

Cuzzi J.N. and Estrada P.R. 1998. Compositional evolution of saturn's rings due to meteoroid bombardment. Icarus 132:1–35.

Dougherty M. and Esposito L. 2009. Saturn from Cassini-Huygens. Springer Science and Business Media.

Elliot J.L., Dunham E., and Mink D. 1977. The rings of Uranus. Nature267:328–330.

Estrada P.R., Durisen R.H., Cuzzi J.N., and Morgan D.A. 2015. Combined structural and compositional evolution of planetary rings due to micrometeoroid impacts and ballistic transport. Icarus252:415–439.

Fortney J.J., Marley M.S., and Barnes J.W. 2007. Planetary Radii across Five Orders of Magnitude in Mass and Stellar Insolation: Application to Transits. APJ659:1661–1672.

Galilei G. 1989. Sidereus nuncius, or, The Sidereal messenger. Chicago : University of Chicago Press, 1989.

Harris A.W. 1984. The origin and evolution of planetary rings. *In* IAU Colloq. 75: Planetary Rings, pages 641–659.

Hayashi C. 1981. Structure of the Solar Nebula, Growth and Decay of Magnetic Fields and Effects of Magnetic and Turbulent Viscosities on the Nebula. Progress of Theoretical Physics Supplement 70:35–53.

Hedman M.M. 2015. Why are dense planetary rings only found between 8 AU and 20 AU? ArXiv e-prints .

Kenworthy M.A. and Mamajek E.E. 2015. Modeling giant extrasolar ring systems in eclipse and the case of J1407b: sculpting by exomoons? ArXiv e-prints .

Mamajek E.E., Quillen A.C., Pecaut M.J., Moolekamp F., Scott E.L., Kenworthy M.A., Collier Cameron A., and Parley N.R. 2012. Planetary Construction Zones in Occultation: Discovery of an Extrasolar Ring System Transiting a Young Sun-like Star and Future Prospects for Detecting Eclipses by Circumsecondary and Circumplanetary Disks. AJ143:72.

Maxwell J.C. 1856. Stability of the Motion of Saturn's Rings.

Nicholson. 2000. Saturn's rings i: Optical depth profiles from the 28 sgr occultation. Icarus 145:474 – 501.

Northrop T. and Connerney J. 1987. A micrometeorite erosion model and the age of saturn's rings. Icarus 70:124–137.

Ockert-Bell M.E., Burns J.A., Daubar I.J., Thomas P.C., Veverka J., Belton M.J.S., and Klaasen K.P. 1999. The Structure of Jupiter's Ring System as Revealed by the Galileo Imaging Experiment. Icarus 138:188–213.

Ohta Y., Taruya A., and Suto Y. 2009. Predicting photometric and spectroscopic signatures of rings around transiting extrasolar planets. The Astrophysical Journal 690:1.

Ortiz J.L., Duffard R., Pinilla-Alonso N., Alvarez-Candal A., Santos-Sanz P., Morales N., Fernández-Valenzuela E., Licandro J., Campo Bagatin A., and Thirouin A. 2015. Possible ring material around centaur (2060) Chiron. A&A576:A18.

Owen T., Danielson G.E., Cook A.F., Hansen C., Hall V.L., and Duxbury T.C. 1979. Jupiter's rings. Nature281:442–446.

Pilcher C.B., Chapman C.R., Lebofsky L.A., and Kieffer H.H. 1970. Saturn's rings: Identification of water frost. Science 167:1372–1373.

Pollack J.B., Grossman A.S., Moore R., and Graboske Jr. H.C. 1976. The formation of Saturn's satellites and rings, as influenced by Saturn's contraction history. Icarus29:35–48.

Ruprecht J.D., Bosh A.S., Person M.J., Bianco F.B., Fulton B.J., Gulbis A.A.S., Bus S.J., and Zangari A.M. 2015. 29 November 2011 stellar occultation by 2060 Chiron: Symmetric jet-like features. Icarus252:271–276.

Schlichting H.E. and Chang P. 2011. Warm Saturns: On the Nature of Rings around Extrasolar Planets That Reside inside the Ice Line. APJ734:117.

Seager S., Kuchner M., Hier-Majumder C.A., and Militzer B. 2007. Mass-Radius Relationships for Solid Exoplanets. APJ669:1279–1297.

Sing D.K. 2010. Stellar limb-darkening coefficients for CoRot and Kepler. A&A510:A21.

Smith B.A., Soderblom L.A., Banfield D., Barnet C., Beebe R.F., Bazilevskii A.T., Bollinger K., Boyce J.M., Briggs G.A., and Brahic A. 1989. Voyager 2 at Neptune - Imaging science results. Science 246:1422–1449.

Spahn F., Schmidt J., Albers N., Hörning M., Makuch M., Seiß M., Kempf S., Srama R., Dikarev V., Helfert S., *et al*. 2006. Cassini dust measurements at enceladus and implications for the origin of the e ring. Science 311:1416–1418.

Thiessenhusen K.U., Krivov A., Krüger H., and Grün E. 2002. A dust cloud around pluto and charon. Planetary and Space Science 50:79–87.

Tiscareno M.S. 2013. Planetary Rings, page 309.

Tusnski L.R.M. and Valio A. 2011. Transit model of planets with moon and ring systems. The Astrophysical Journal 743:97.

Zuluaga J.I., Kipping D., Sucerquia M., and Alvarado J.A. 2015. A novel method for identifying exoplanetary rings. ArXiv e-prints .